PHILOSOPHICAL TRANSACTIONS OF THE ROYAL SOCIETY A MATHEMATICAL, PHYSICAL & ENGINEERING SCIENCES

Light Scattering in the Study of Dynamical Properties

E. R. Pike

Phil. Trans. R. Soc. Lond. A 1979 **293**, 349-358
doi: 10.1098/rsta.1979.0102

Phil. Trans. R. Soc. Lond. A **293**, 349–358 (1979)
Printed in Great Britain

Light scattering in the study of dynamical properties

By E. R. Pike
Royal Signals and Radar Establishment, Malvern, Worcestershire WR14 3PS, U.K.

[Plate 1]

Motion in many forms may be studied by light scattering. On one extreme this may be the bulk motion of a large target such as a vehicle or a satellite; on the other it may be the diffusional motion of an atom or molecule. The paper will outline the basic principles involved in such measurements and introduce the mathematical apparatus required to derive spectra of the scattered light. This can be couched in terms of speckle and Doppler shifts in the first case, while for molecular systems in thermodynamic equilibrium, we need a form of modern many-body theory. With this we calculate dynamical mode correlations as functions of the transport coefficients of irreversible thermodynamics. Examples will be given in the measurement of flow and turbulence, marcromolecular diffusion and polydispersity, and molecular scattering, including mode–mode coupling effects in condensed matter.

I wish to illustrate some of the complexities of the subject of interactions and dynamics by reference to figure 1. First, we look at the light scattered when a laser is taken off the shelf and pointed at a surface (piece of paper) in uniform translation. The result is seen to be a cloud of tiny 'speckles' moving in the same direction as the surface (figure 1*a*). A different laser, under apparently identical circumstances, will produce speckles of a different size moving with a different velocity. The size of the speckles, in fact, is a function of the beam size, and the velocity is dependent upon the wavefront curvature. If we insert a lens into the beam we can change both these factors and, as the original diverging laser beam is brought to a focus at the surface, the pattern slows down its translation and the speckle size increases (figure 1*b*) until at focus the wavefront is planar and the beam size at its minimum when the pattern stops translating, with large speckles (figure 1*c*) just evolving on the spot. The lifetime of the speckles is related to the transit time of the scatterer through the beam. As the lens is brought even closer to the surface the speckles decrease in size again and start moving in the opposite direction.

The second sequence shows how the scattered light would behave if the beam were focused at a point where two separate velocities are present. A real example would be light scattering from superfluid ^{4}He, where two first-sound waves propagating in opposite directions create the scattering. Here we see (shown in a cine film in the original presentation) that, instead of the speckles evolving with a given lifetime, which in this case would be the phonon lifetime, the individual speckles flash on and off a number of times before they disappear. The two frequencies present in a given scattering direction clearly beat together at a frequency given by the difference between them.

So far we have had a large enough beam, compared with the scale of the scatterer, to encompass many scattering centres, and have made our observations in the far field. The speckle pattern in these cases gives no information about the spatial structure of the medium.

In the next examples we have moved into the near field of a random scatterer and observe quite different behaviour. Instead of speckles we have a faint 'swimming-pool' type of pattern where connected lines of caustics with associated fringe patterns move across the field of view (figure 1*d*). This is the type of pattern created, for example, by starlight falling on the earth through the turbulent atmosphere. In figure 1*e* we have moved further away into the so-called focusing region where the effects are strongest, and away into the far field the sequence ends with the Gaussian speckle again (figure 1*f*). The mathematical description of these scattered light fields requires a mixture of diffraction theory and quantum statistics which is yet in its early stages and the rich variety of phenomena to be exploited in this way is still growing.

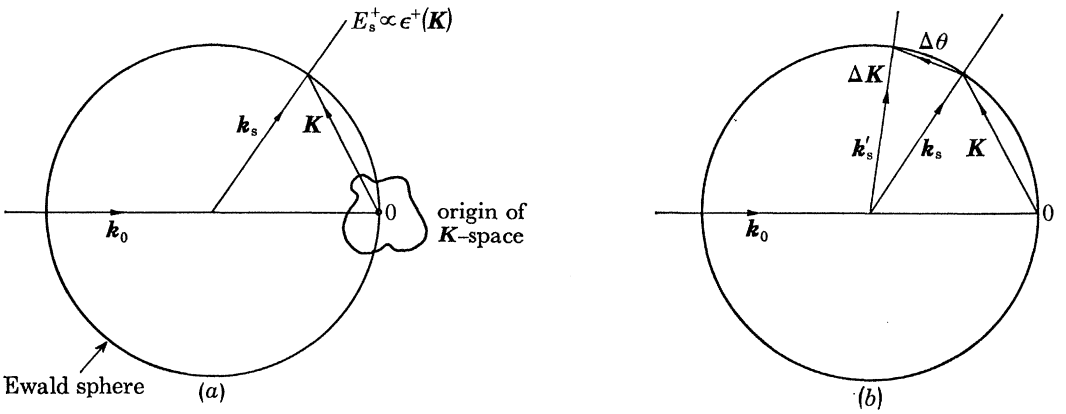

FIGURE 2. Ewald sphere construction (*a*) for scattered field, (*b*) for coherence criterion.

In this paper I cannot review the field in any great detail. I have decided therefore to concentrate on presenting the mathematical theory required to tackle some of these problems, but will also show some selected applications and results.

The basic diffraction effects are best approached using the theory of Einstein–Smoluchowski. We consider only the so-called Rayleigh–Gans–Debye approximation in which multiple scattering effects are ignored. Dr Gelbart will be dealing with these in a later contribution.

The light scattered from a distribution of stationary particles in a given scattering direction is shown by this theory to be linearly related to a Fourier component of spatially varying dielectric susceptibility tensor. For small spherical scatterers, for example, this would be a Fourier component of the density distribution. We normally deal with the positive frequency part of the field $E^+(\boldsymbol{r}, t)$ as $|E^+|^2$ gives rise to the photodetection probability.

The familiar Ewald sphere construction can be used, with the dielectric susceptibility taking the role of reciprocal space density (figure 2*a*). With the notation of the figure, the scattering wavevector is defined as

$$\boldsymbol{K} = \boldsymbol{k}_s - \boldsymbol{k}_0, \tag{1}$$

and

$$E_s^+(\boldsymbol{K}) = \sum_i \epsilon(\boldsymbol{r}_i) \exp(-\mathrm{i}\boldsymbol{K}\cdot\boldsymbol{r}_i) = \epsilon(\boldsymbol{K}). \tag{2}$$

The speckle pattern can be understood by considering scattering from two equal separated fluctuations at $\boldsymbol{r}_1$ and $\boldsymbol{r}_2$ respectively. By using the Ewald sphere we see that in the direction k_s we have

$$E_s^+(\boldsymbol{K}) \propto \Delta\epsilon(\boldsymbol{K}) \propto \exp(\mathrm{i}\boldsymbol{K}\cdot\boldsymbol{r}_1) + \exp(\mathrm{i}\boldsymbol{K}\cdot\boldsymbol{r}_2). \tag{3}$$

The intensity is thus

$$|E^+(\boldsymbol{K})|^2 = \text{constant} + \exp\{\mathrm{i}\boldsymbol{K}\cdot(\boldsymbol{r}_1 - \boldsymbol{r}_2)\} + \text{c.c.} \tag{4}$$

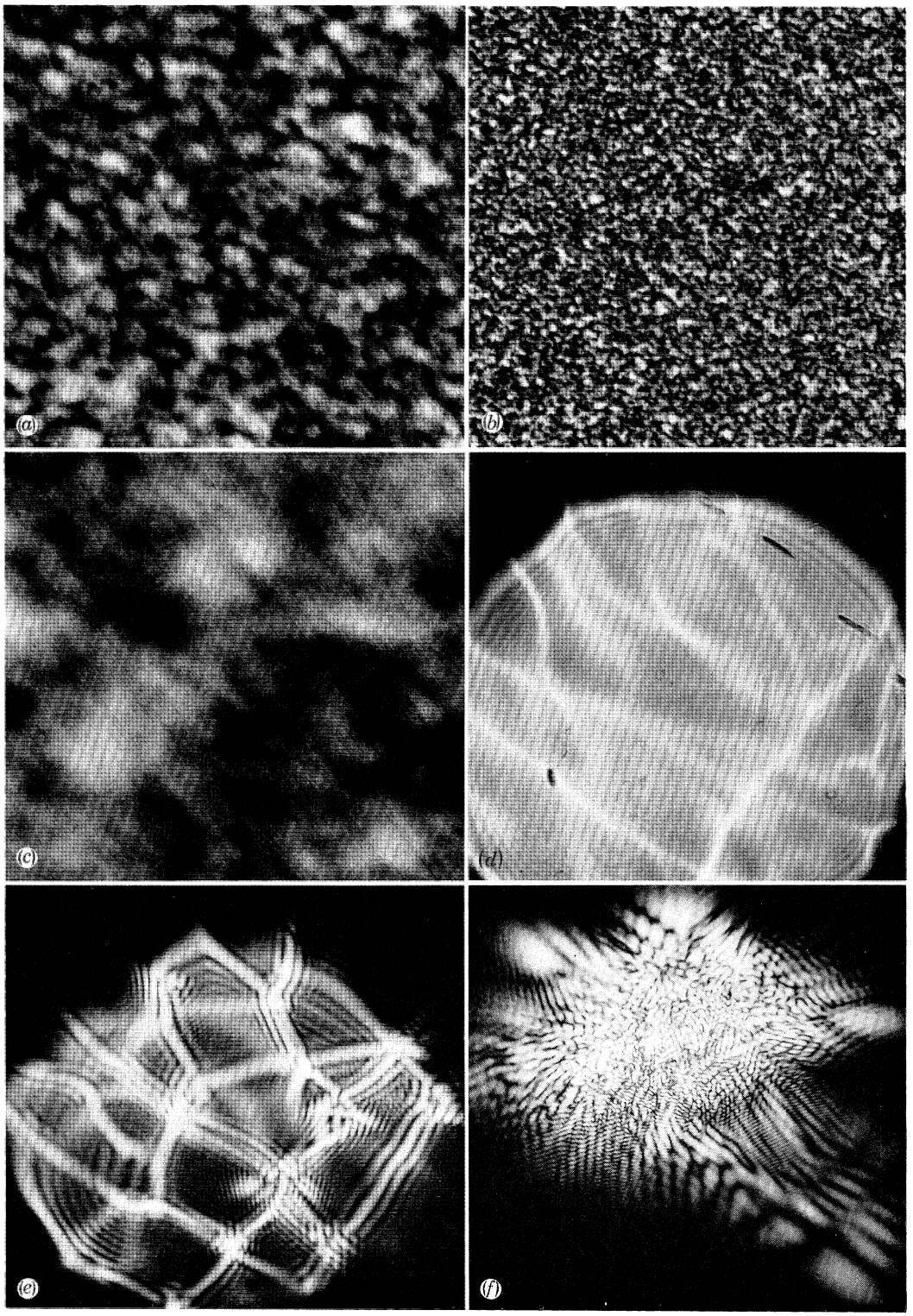

FIGURE 1. Speckle patterns described in the text.

(*Facing p.* 350)

PHILOSOPHICAL TRANSACTIONS OF THE ROYAL SOCIETY A MATHEMATICAL, PHYSICAL & ENGINEERING SCIENCES

In a second scattering direction $\boldsymbol{k}_s'$, the scattering vector is $\boldsymbol{K}+\Delta\boldsymbol{K}$ (figure 2*b*) and the scattered intensity is

$$|E^+(\boldsymbol{K}+\Delta\boldsymbol{K})|^2 = \text{constant} + \exp\{\mathrm{i}(\boldsymbol{K}+\Delta\boldsymbol{K})\cdot(\boldsymbol{r}_1-\boldsymbol{r}_2)\} + \text{c.c.} \tag{5}$$

These will add in phase or 'coherently' if, say,

$$\Delta\boldsymbol{K}\cdot(\boldsymbol{r}_1-\boldsymbol{r}_2) < 2\pi. \tag{6}$$

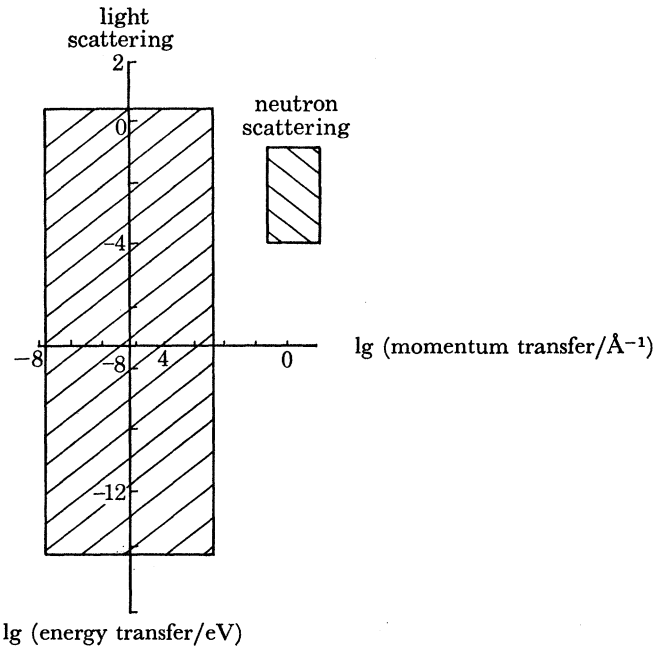

FIGURE 3. The ranges of energy and momentum transfer for light and neutron scattering.

Let us denote the maximum projection of $\boldsymbol{r}_1-\boldsymbol{r}_2$ over all points of the scatterer on $\boldsymbol{K}$ by d. Then for coherent detection we must have

$$\Delta\boldsymbol{K}d < 2\pi. \tag{7}$$

From the Ewald construction we see that

$$\Delta\theta = \Delta\boldsymbol{K}/k. \tag{8}$$

So that the coherence condition is the diffraction criterion:

$$\Delta\theta < \lambda/d. \tag{9}$$

The range of momentum and energy transfers covered by the light scattering technique is shown in figure 3, where they are compared with neutron scattering. The Einstein–Smoluchowski formula can be generalized if the local fluctuations of dielectric constant are in motion. If we follow the fluctuation at $\boldsymbol{r}_1$ which moves instantaneously at velocity $\boldsymbol{v}$, the phase $\boldsymbol{K}\cdot\boldsymbol{r}_1$ becomes $\boldsymbol{K}\cdot(\boldsymbol{r}_{01}+\boldsymbol{v}t)$ which gives a frequency (Doppler) shift of $\boldsymbol{K}\cdot\boldsymbol{v}$. For a set of fluctuations moving with velocity $\boldsymbol{v}$,

$$E_s(\boldsymbol{K}, t) = \{\sum_i \epsilon(\boldsymbol{r}_i)\exp(\mathrm{i}\boldsymbol{K}\cdot\boldsymbol{r}_{0i})\}\exp(\mathrm{i}\boldsymbol{K}\cdot\boldsymbol{v}t). \tag{10}$$

Such Doppler shifts with coherent detection are used in radar-type applications of light scattering. In figure 4 we show a record of the motion of the atmosphere in a vortex behind a large aircraft obtained in this way by workers at R.S.R.E. (see Pike 1976) the scattering particles are natural aerosols. Figure 5 shows the same experiment used for measuring retinal blood flow (Hill *et al.* 1977).

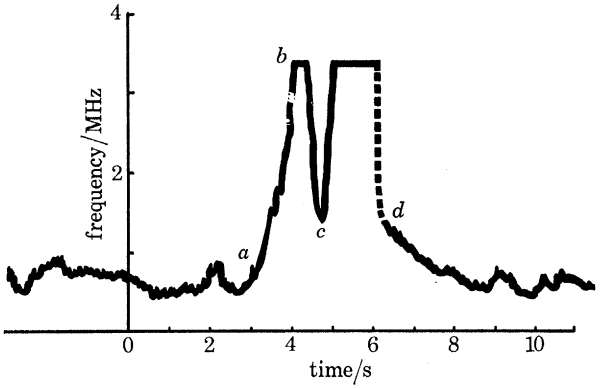

FIGURE 4. Motion of atmosphere behind a VC10 aircraft landing.

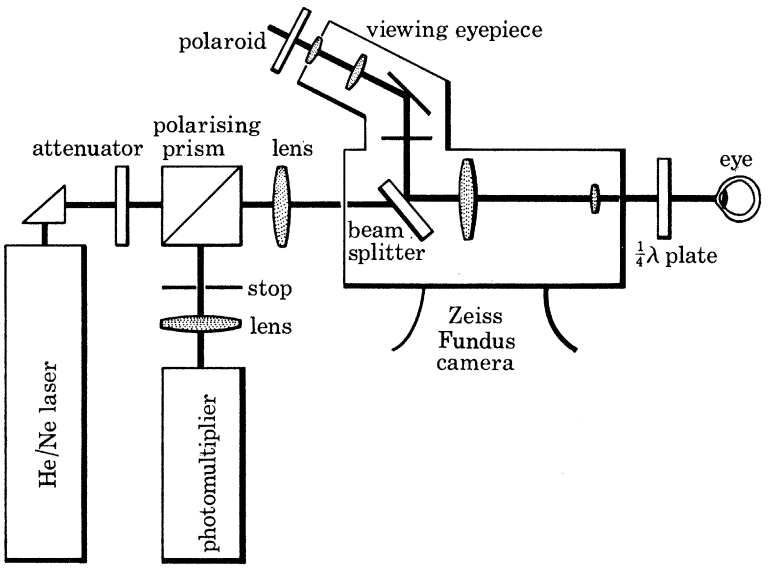

FIGURE 5. Block schematic of retinal blood flow measurement apparatus.

A widely used variant of the plain Doppler shift is known as the differential Doppler method. Here two incident laser beams are crossed at the required location and the detector sees Doppler shifts from each beam:

$$\omega_1 = (\boldsymbol{k}_s - \boldsymbol{k}_{01}) \cdot \boldsymbol{v} \text{ rad s}^{-1}, \tag{11}$$

$$\omega_2 = (\boldsymbol{k}_s - \boldsymbol{k}_{02}) \cdot \boldsymbol{v} \text{ rad s}^{-1}. \tag{12}$$

The output of the detector has the difference frequency

$$\omega = \omega_1 - \omega_2 = (\boldsymbol{k}_{02} - \boldsymbol{k}_{01}) \cdot \boldsymbol{v}, \tag{13}$$

which has the desirable feature of being independent of scattering direction. If only one particle at a time is present in the scattering volume so that averaging over speckles does not occur, a large-aperture receiver can be used with a consequent gain in light collection.

Figure 6 shows an experiment of this type in a supersonic wind tunnel. The complex nature of the interaction between a normal shock wave and a boundary layer is mapped out (Abbiss *et al.* 1976). A minute quantity of small oil droplets was introduced to provide the scattering 'seed' particles.

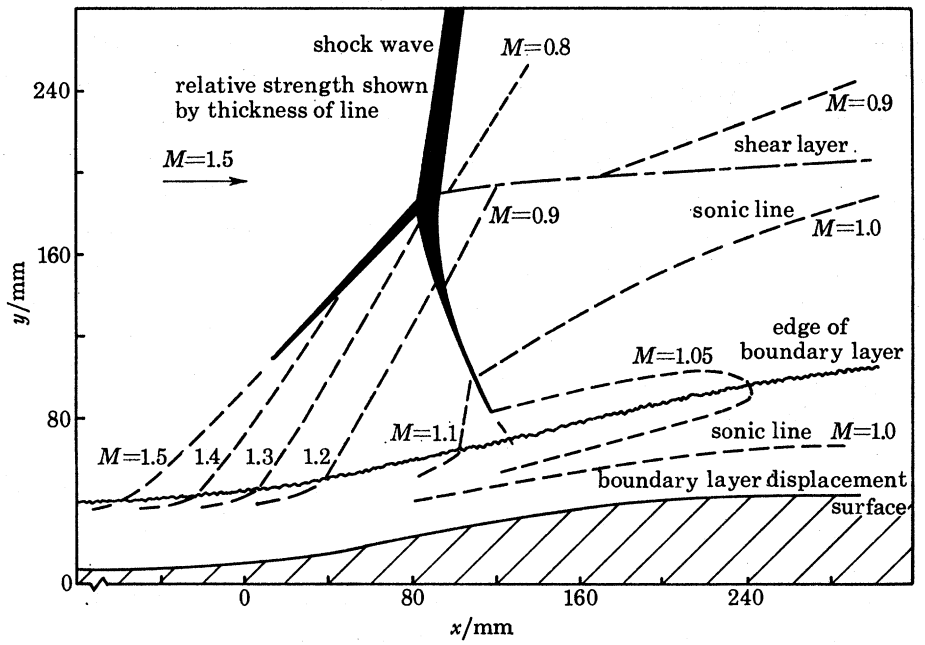

FIGURE 6. Velocity contours in normal-shock – boundary-layer interaction.

Turbulence can be studied either by scattering from the related refractive index fluctuations or from 'seed' particles following the velocity fluctuations.

For more general time dependencies than those given by pure translation, the behaviour of the time-varying quantities, for a polarized incident wave in the Cartesian direction β,

$$E_\alpha^+(\boldsymbol{K}, t) \propto \int \epsilon_{\alpha\beta}(\boldsymbol{r}) \exp(\mathrm{i}\boldsymbol{K}\cdot\boldsymbol{r}(t))\, \mathrm{d}^3\boldsymbol{r} = \epsilon_{\alpha\beta}(\boldsymbol{K}, t), \tag{14}$$

are required.

The optical spectrum of this field is defined:

$$\begin{aligned} S(\boldsymbol{K}\omega) &= \left\langle \lim_{T\to\infty} \left| \frac{1}{T} \int_{-\frac{1}{2}T}^{\frac{1}{2}T} E^+(\boldsymbol{K}, t) \exp(-\mathrm{i}\omega t)\, \mathrm{d}t \right|^2 \right\rangle \\ &= \lim_{T\to\infty} \frac{1}{T} \int_{-\frac{1}{2}T}^{\frac{1}{2}T} \int_{-\frac{1}{2}T}^{\frac{1}{2}T} \langle E^+(\boldsymbol{K}, t)\, E^-(\boldsymbol{K}, t')\rangle \exp(-\mathrm{i}\omega(t-t'))\, \mathrm{d}t\, \mathrm{d}t', \end{aligned} \tag{15}$$

where the angle brackets denote an ensemble average. For a stationary process this reduces to

$$S(\boldsymbol{K}\omega) = \int_{-\infty}^{+\infty} G^{(1)}(\tau) \exp(-\mathrm{i}\omega\tau)\, \mathrm{d}\tau, \tag{16}$$

where

$$G^{(1)}(\tau) = \langle E^+(\boldsymbol{K}, \tau)\, E^-(\boldsymbol{K}, 0)\rangle \tag{17}$$

is the first order correlation function of the electric field. Thus,

$$G^{(1)}(\tau) \propto \langle \epsilon_{\alpha\beta}^+(\boldsymbol{K}, t)\, \epsilon_{\alpha\beta}(\boldsymbol{K}, 0)\rangle. \tag{18}$$

The calculation of light scattering spectra, therefore, amounts to the evaluation of the spectra or correlation functions of the dielectric susceptibility fluctuations. These must then be related to the fluctuations of the variables causing the dielectric perturbations. These variables can be of many kinds, either microscopic or macroscopic. Each such variable, by the Curie principle, gives rise to scattering phenomena characteristic of its own particular tensorial order and symmetry. We can distinguish, for example, Rayleigh scattering (in its present-day connotation) as due to entropy fluctuations at constant pressure, Brillouin scattering as due to transverse and longitudinal first sound pressure fluctuations at constant entropy, Raman scattering as due to scattering from optic phonons, magnon scattering from spin waves etc.

The calculation of the spectra of such variables for systems in thermodynamic equilibrium is a central problem in modern quantum and classical statistical mechanics. It is best to tackle any particular problem by first breaking it down, by symmetry considerations, into decoupled irreducible parts. In any given symmetry, one then has a number of processes which will usually be coupled amongst themselves. These interacting dynamical modes then present to the physicist a problem of coupled fields familiar in its microscopic form in elementary particle theory and many-body theory. The mathematical apparatus used is that of the thermodynamic propagator or Green function and its hierarchy of equations or Feynman diagrams. The coupled-mode problem of electrons and phonons in a superconductor is a familiar example of a striking success for these theories.

It was shown in the late 1950s that the Green functions were the response functions or transport coefficients of irreversible thermodynamics in the first Born approximation of perturbation theory (Zubarev 1960). The thermodynamic Green function in its analytic or 'double-time' form is a Fourier–Hilbert transform into a complex energy domain of the correlation function and also gives immediately the spectrum of the variable concerned. The wavevector and frequency-dependent propagator equations are used because they are algebraic as distinct from the differential or integro-differential equations for spectra or correlation functions. The (normalized) Green function for a single variable A, say, has the form

$$g_A(E) = 1/(E - l_A), \tag{19}$$

where l_A is the (in general complex) 'self-energy' of the mode and, of course, in its dependence on wavevector and energy reflects all the dynamics of the system. For simple relaxation it is a purely imaginary number, while for a propagating mode it will have a real part. An example of the former case is that of diffusion of spherical macromolecules in dilute solution. The Green function takes the form

$$g_A = 1/(E - \mathrm{i}DK^2), \tag{20}$$

where D is the translational diffusion coefficient. The spectrum is a Lorentzian centred at the laser frequency and the correlation function is a decaying exponential. The spectrum is usually too narrow to resolve with interferometric spectrometry, and the correlation of fluctuations of intensity (the evolving speckle) is normally measured with a photon correlator. A typical result is shown in figure 7 where the diffusion constants of polymer coated particles are determined. The coating thickness can be measured as a function of polymer concentration in the forming process (A. Smith, Unilever, unpublished).

In cases of polydispersity a sum of exponentials is obtained. This is essentially the Laplace transform of the distribution of molecular sizes. Low-order moments of this distribution can be obtained in many cases and in recent work at Malvern we have shown by a generalization of

PHILOSOPHICAL TRANSACTIONS OF THE ROYAL SOCIETY A MATHEMATICAL, PHYSICAL & ENGINEERING SCIENCES

Shannon's information theory how to invert the Laplace transform much more effectively than has been possibly previously (McWhirter & Pike 1978).

For a system of coupled modes the formula for the Green function is generalized to the matrix Dyson equation (Pike 1974),

$$g = [E - l]^{-1}, \tag{21}$$

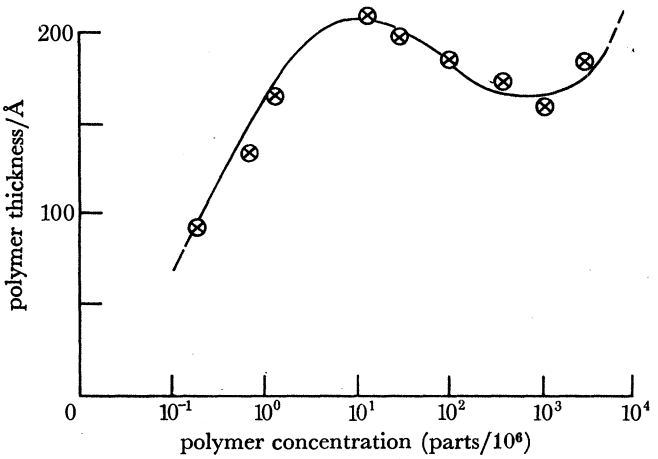

FIGURE 7. Thickness of polymer coatings determined by light scattering from Brownian motion.

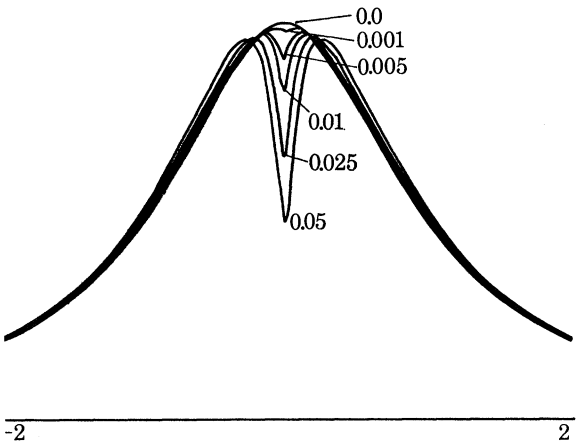

FIGURE 8. Two coupled modes: spectrum as a function of coupling strength. $\Gamma = 1.0; \gamma = 0.05; v_1 = 0; v_2 = 0.$

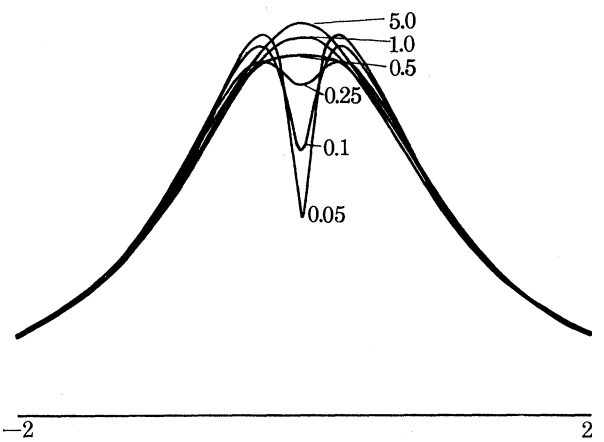

FIGURE 9. Two coupled modes: spectrum as a function of one of the linewidths. $\Gamma = 1.0; \gamma = 0.05; v_1 = 0; v_2 = 0.$

where the quantities are matrices. The l is the 'bare' self-energy matrix and the diagonal self-energy l_A is now a function of these 'bare' quantities. For example, for two interacting modes A and B it can be shown that

$$l_A = l_{AA} - l_{AB}\, l_{BA}\, g_{BB} \tag{22}$$

is the exact renormalized or 'dressed' self-energy of mode A. This result follows directly from equation (74) of Pike (1974) and generalizes equation (123) of that paper.

The amount of physics contained in this beautifully simple result is quite remarkable. In figures 8–10 we have calculated spectra for various (non-dispersive, local) values of the bare coefficients. The coupling $l_{AB}\, l_{BA}$ is denoted by c, l_{AA} by $v_1 + i\Gamma$ and l_{BB} by $v_2 + i\gamma$.

PHILOSOPHICAL TRANSACTIONS OF THE ROYAL SOCIETY A MATHEMATICAL, PHYSICAL & ENGINEERING SCIENCES

We can easily obtain the theory of the Mountain line (Mountain 1966), the v.h. depolarized scattering of anisotropic liquids (Stegeman & Stoicheff 1968), and Kawasaki–Ferrell theory of critical scattering and a number of other phenomena. As a matter of fact, the result (22) for non-propagating interacting modes was already published in 1958 in Landau & Lifschitz (1958). In their notation† we have for the cross-spectral density of two variables:

$$\langle x_i\, x_k \rangle = \operatorname{Im} \alpha_{ik}, \tag{23}$$

where

$$\alpha_{ik} = T^{-1}(\beta_{ik} - \mathrm{i}\omega\gamma_{ik}^{-1})^{-1}. \tag{24}$$

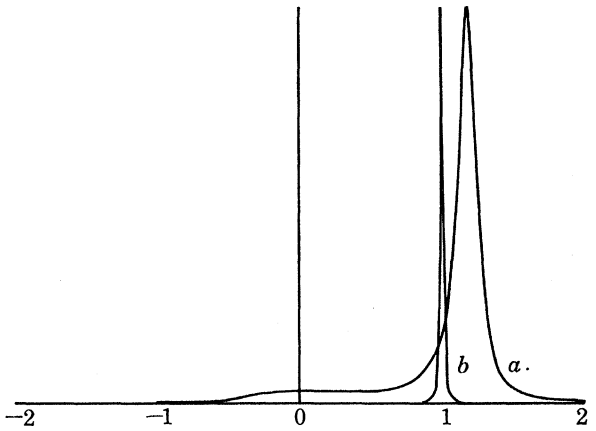

FIGURE 10. The effect of a non-propagating mode on a sharp propagating one. $\Gamma = 0.01$; $\gamma = 0.5$; $c = 0.25$ (a); $c = 0.0$ (b).

The β's are static susceptibilities given by the entropy fluctuation:

$$S - S_0 = -\tfrac{1}{2} \sum_{ik} \beta_{ik} x_i x_k. \tag{25}$$

The γ's are transport coefficients given by generalized fluxes:

$$\dot{x}_i = -\gamma_{ik} X_k, \tag{26}$$

where the X's are generalized forces,

$$X_k = \beta_{kj} x_j. \tag{27}$$

In the chemical literature classical versions of these field theories have been pursued over the last two decades with, unfortunately, minimal contact with theoretical physics. Based on the Liouville rather than the Hamiltonian operator and sometimes called the 'Zwanzig–Mori formalism' they have now successfully reproduced, for example, the Landau–Lifschitz formula in theories of the above-mentioned depolarized light scattering from anisotropic liquids. In this case x_i would be the molecular orientation density and x_j the vorticity or transverse momentum density.

A final two-variable example, in which the self energies are non-local and dispersive, is the recent work of Sandercock (1978) on the scattering from surface ripples on metals. The 'A' variable is the longitudinal phonon and the 'B' variable the transverse wave with polarization in the plane of the scattering vector and perpendicular to the surface. The coupling is provided by the boundary constraints on the stress.

† To compare with Mountain (1966): $\alpha = -M/(kTE)$, $\beta = kN^{-1}$, $k\gamma = L$.

For this case the Green function has been calculated by Loudon (1978) to be

$$g_{u_z u_z} \propto \frac{E l_X l_L}{(E^2 - l_X^2)^2 + l_X^2 l_L l_T}, \tag{28}$$

where

$$l_S = 2^{\frac{1}{2}} v_T q_S, \quad S = X, L, T, \tag{29}$$

v_T being the transverse wave velocity and the q_S being the momentum transfers along the surface by the longitudinal and by the transverse waves respectively. The agreement between theory and experiment is shown in figure 11.

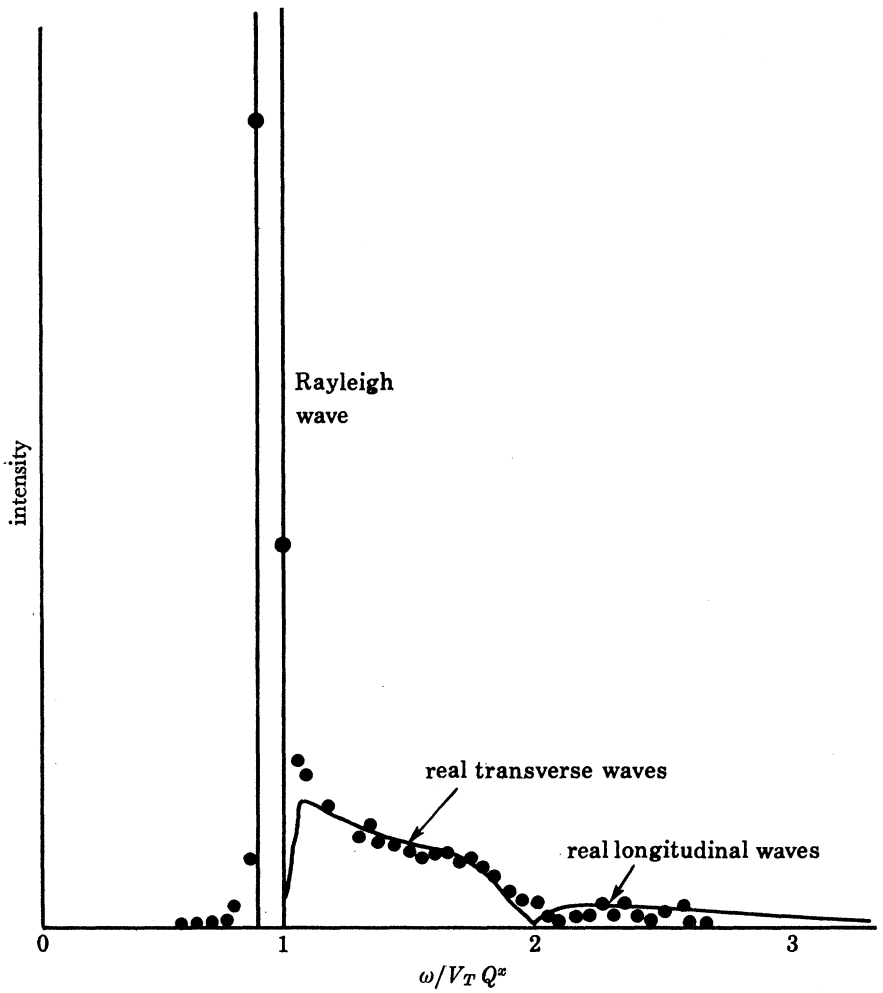

FIGURE 11. The scattering from surface ripples on aluminium. ——, Theory (Loudon 1978; ●, experiment (Sandercock 1978).

In summary, the study of interactions and dynamics of physical, chemical and biological systems by light scattering is a powerful and thriving field of great depth, with continuing potential for a large number of diverse applications.

PHILOSOPHICAL TRANSACTIONS OF THE ROYAL SOCIETY A MATHEMATICAL, PHYSICAL & ENGINEERING SCIENCES

References (Pike)

Abbiss, J. B., East, L. F., Nash, C. R., Parker, P., Pike, E. R. & Sawyer, W. G. 1976 *A study of the interaction of a normal shock wave and a turbulent boundary layer using a laser anemometer*. R.A.E. Technical Report 75141.
Hill, D. W., Parker, P., Pike, E. R. & Young, S. 1977 *IEEE J. Quantum Electron.* QE–**13**, D85.
Landau, L. D. & Lifschitz, E. M. 1958 *Statistical physics*, ch. 12. Oxford: Pergamon Press.
Loudon, R. 1978 *Phys. Rev. Lett.* **40**, 581.
McWhirter, J. G. & Pike, E. R. 1978 *J. Phys* A **11**, 1729.
Mountain, R. D. 1966 *J. Res. natn. Bur. Stand.* A**70**, 207.
Pike, E. R. 1974 *Photon correlation and light beating spectroscopy* (ed. E. R. Pike & H. Z. Cummins) New York: Plenum Press.
Pike, E. R. 1976 *The engineering uses of coherent optics* (ed. E. R. Robertson), p. 450. Cambridge University Press.
Sandercock, J. 1978 *Solid St. Commun.* **26**, 547.
Stegeman, G. I. A. & Stoicheff, B. P. 1968 *Phys. Rev. Lett.* **21**, 202.
Zubarev, D. N. 1960 *Soviet Phys. Usp.* **3**, 321.

PHILOSOPHICAL TRANSACTIONS OF THE ROYAL SOCIETY A MATHEMATICAL, PHYSICAL & ENGINEERING SCIENCES

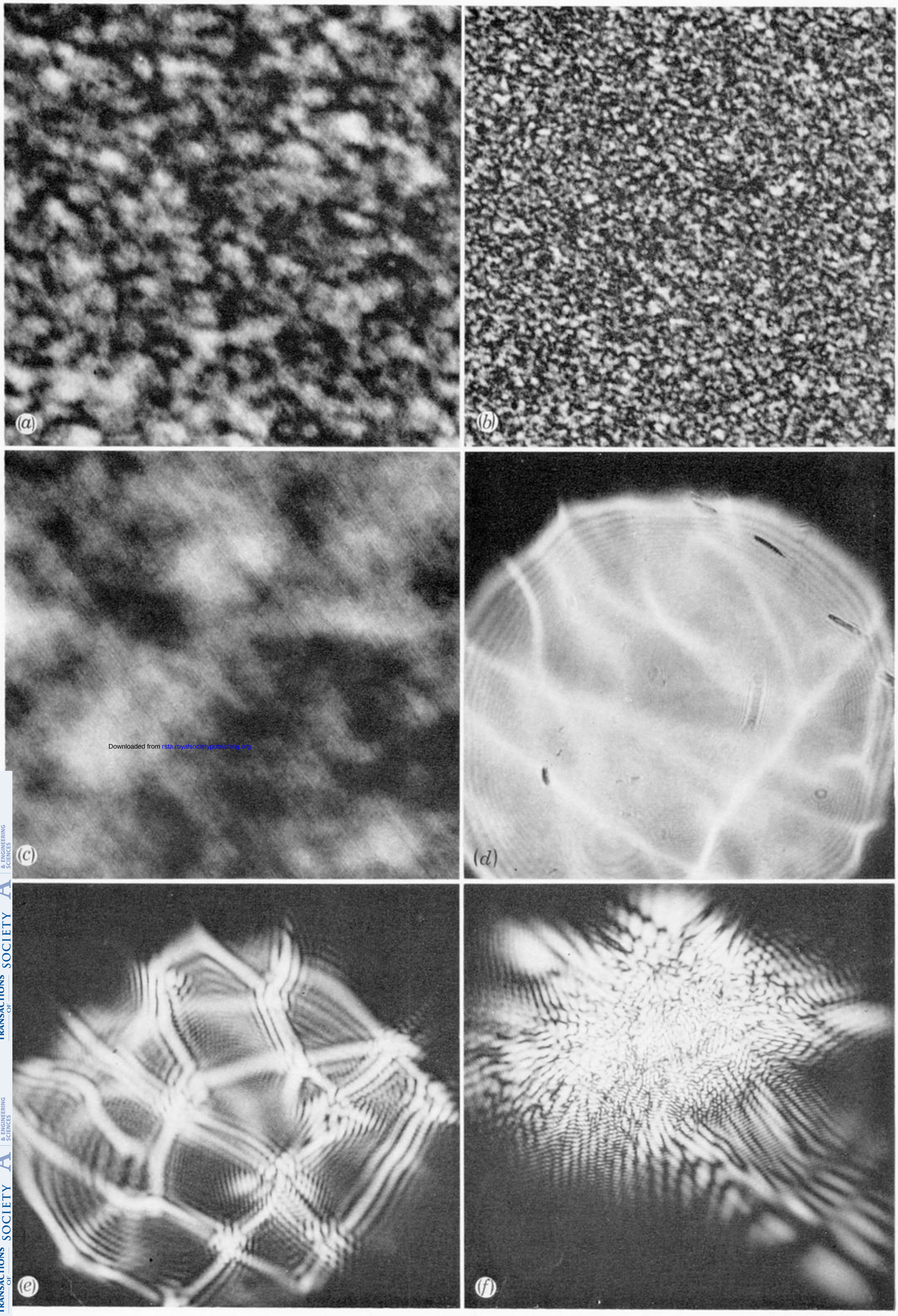

FIGURE 1. Speckle patterns described in the text.